Prebiotic protocell membranes retain encapsulated contents during flocculation, and phospholipids preserve encapsulation during dehydration

Zachary R. Cohen<sup> $l^{\dagger}_{+}$ \*</sup>, Caitlin. E. Cornell $l^{\dagger}$ , David C. Catling $^{2^{\dagger}_{+}}$ , Roy A. Black<sup>l</sup>, Sarah L. Keller $^{l^{\dagger}_{+}}$ .

<sup>1</sup>Department of Chemistry, University of Washington, Seattle WA 98195, USA.

<sup>2</sup>Department of Earth and Space Sciences, University of Washington, Seattle WA 98195, USA.

<sup>‡</sup>Astrobiology Program, University of Washington, Seattle WA 98195, USA.

KEYWORDS: Prebiotic chemistry, origin of life, vesicle, fatty acid, flocculation.

#### ABSTRACT:

The first cell membranes were likely composed of single chain amphiphiles such as fatty acids. An open question is whether fatty acid membranes could have functioned within evaporative lakes on the early Earth, which have been hypothesized to concentrate prebiotic reactants. Evaporation also concentrates monovalent salts, which in turn cause fatty acid membrane vesicles to flocculate; significant loss of encapsulated contents during flocculation would have impeded early cell evolution. Here, we tested whether fatty acid vesicles retain encapsulated contents after flocculation and after drying. We found that vesicles composed of 2:1 decanoic acid: decanol encapsulate calcein dye throughout a process of flocculation in saturated salt solution and subsequent disaggregation of vesicles by dilution of the salt. However, 30-minutes of complete dehydration disrupted encapsulation by fatty acid vesicles. In contrast, phospholipid vesicles maintained encapsulation. Our results reveal a selective pressure for protocells to incorporate

phospholipids: while fatty acid membranes can retain encapsulated contents during periods of dilute and saturating salt, phospholipids are necessary for encapsulation during dry periods. Our results are consistent with the hypothesis that evaporative lakes were productive sites for prebiotic chemistry and the origin of cells.

#### INTRODUCTION:

Compartmentalization is necessary for cells. It allows genetic material to be sequestered and metabolite concentrations to be regulated. The earliest protocells were likely separated from their environment by a membrane of fatty acids<sup>1</sup> that were delivered to Earth via meteorites<sup>2</sup> or synthesized locally via Fischer-Tropsch<sup>3</sup> or sparking reactions<sup>4</sup>.

A protocell is typically depicted as a single vesicle enclosing an interior solution<sup>5–7</sup>, as in Fig 1a. If the vesicle is made of fatty acids, it is stable over a limited range of solution pH values within about half a unit of the effective pKa of the fatty acids<sup>8</sup>. If too many fatty acids are charged, only micelles form. If no fatty acids are charged, an oil forms. Even if the pH is conducive to forming vesicles, those vesicles can aggregate into "flocs" (Fig 2a) if the solution has high salt concentration<sup>9</sup>. Flocculation occurs when monovalent cations from the salt screen the negative charges on fatty acids, eliminating electrostatic repulsion between vesicles<sup>10</sup>.

Salty water would have been common on the early Earth, so flocculation of fatty acid vesicles has traditionally been viewed as an obstacle to protocell development<sup>1,11</sup>. Geological evidence suggests that the origin of life on Earth probably occurred before 3.7 Gya<sup>12,13</sup> and that exposed land would have been present at that time<sup>14</sup>. When lakes or ponds form in closed basins (i.e. with no outflow) on terrain made of volcanic rock (i.e. basalt, as expected on the early

Earth<sup>14,15</sup>), the water becomes enriched in dissolved carbonate. The inorganic carbon is derived from atmospheric CO<sub>2</sub> that dissolves in rainwater and then in streams or groundwater to form carbonic acid, which is consumed by reacting with minerals in the catchment rocks, thereby raising the pH and releasing cations that are mainly charge-balanced by bicarbonate<sup>16</sup>. Closed-basin lakes transiently experience saturating salt concentrations during evaporative cycles<sup>17–20</sup>. Evaporative, carbonate-rich lakes are appealing sites for the origin of cells because they can concentrate phosphate and ferrocynanides<sup>19,20</sup>, making them productive sites for prebiotic syntheses that require phosphate, nitriles, or dehydration<sup>21–23</sup>. Therefore, it is worth re-evaluating whether salt-induced flocculation is detrimental. Here we tested whether flocculation prevents vesicles from performing their central role of encapsulating soluble material.

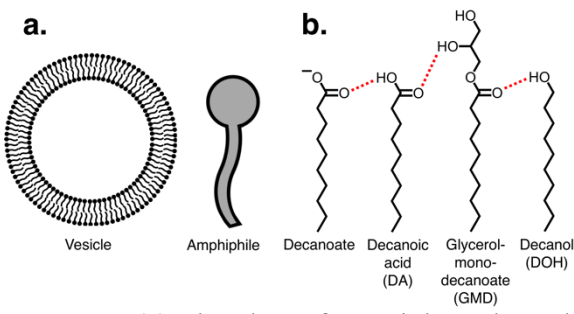


**Figure 1.** (a) Sketches of a vesicle and amphiphile, and (b) structures of prebiotic amphiphiles showing the hydrogen bonding (red dashes) required for bilayer formation.

We produced vesicles from plausibly prebiotic amphiphiles: decanoic acid (DA), decanol (DOH), and glycerol-mono-decanoate (GMD), shown in Fig 1b. Glycerol-monoesters like GMD reduce flocculation at moderate (< 0.6 M NaCl) but not high salt concentrations<sup>11</sup>, as do nucleobases<sup>24</sup> and amino acids<sup>25</sup>. We flocculated vesicles with sodium bicarbonate (NaHCO<sub>3</sub>) and sodium chloride (NaCl), which dissociate into monovalent ions. We did not include divalent cations in our experiments because divalent cations are kept to relatively low concentrations in

natural carbonate-rich lakes due to precipitation of calcium, magnesium, or iron carbonates<sup>26</sup>. On the early Earth, such buffering by carbonate insolubility would keep divalent cations at low (< 2 mM) saturation concentrations<sup>19,20</sup>. Consequently, the relevant aqueous chemistry is dominated by sodium carbonate and chloride, which are highly soluble and can become concentrated during evaporation<sup>19</sup>. In the presence of low concentrations of divalent cations (< 3 mM), fatty acid vesicles maintain encapsulation of small molecules (nucleotides) over long time scales (> 24 hours)<sup>27</sup>.

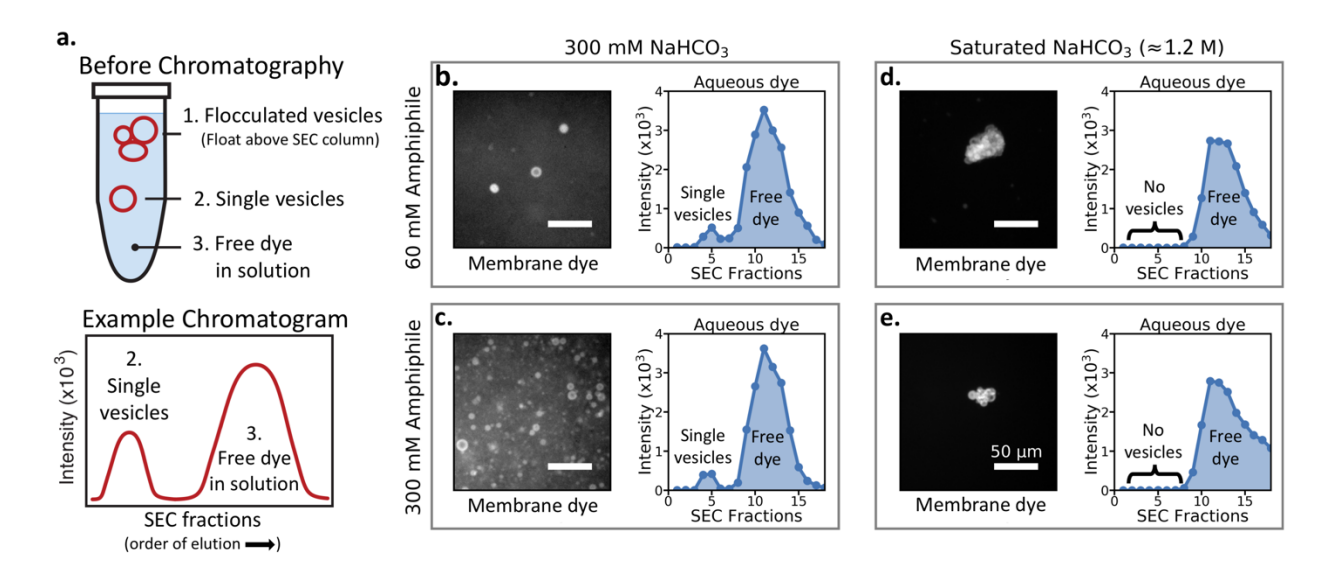


Figure 2. Increasing the concentration of amphiphile does not prevent vesicle flocculation in saturated NaHCO<sub>3</sub> solution. (a) Schematic: in a fatty acid solution, aqueous dye appears in the lumens of flocculated vesicles (1), in single vesicles (2), or free in solution (3). Flocculated vesicles cannot be detected by size-exclusion chromatography (SEC) because their low density prevents them from entering the SEC resin. Single fatty acid vesicles of 4:1:1 DA:DOH:GMD remained dispersed at low salt (b-c) and flocculated in saturated salt (d-e). Images show fluorescence micrographs taken before SEC with a hydrophobic dye that labels membranes (rhodamine 6G). Graphs show SEC chromatograms, which assay larger volumes than micrographs. At low salt concentration (b-c), images and SEC confirm that single vesicles remained dispersed throughout the solution. In saturated salt solution (d-e), only flocculated vesicles appeared in the images, and SEC confirmed that no single vesicles remained. Increasing the concentration of amphiphile did not prevent vesicle flocculation in saturated NaHCO<sub>3</sub> solution. To optimize imaging (which did not change the results) the sample in panel e was diluted 1:1 with SEC running buffer. Scale bars are 50 μm.

#### MATERIALS AND METHODS:

Materials. Decanoic acid was purchased from Nu-Chek Prep (Elysian, MN). Decanol and glycerol-mono-decanoate were purchased from Sigma-Aldrich (St. Louis, MO). DOPC and DOPG were purchased from Avanti Polar Lipids (Alabaster, Al). Bicine, calcein, rhodamine 6G, and carboxyfluorescein were purchased from Sigma-Aldrich (St. Louis, MO). Sepharose 4B was used as the resin for size-exclusion chromatography, and was purchased from Sigma-Aldrich (St. Louis, MO). Triton-X-100 was purchased from Supleco (Bellefonte, PA). Fisherbrand™ 96 - well polystyrene plates (Hanover Park, IL) were used for analyzing samples from size-exclusion chromatography.

Preparation of vesicle solutions. Stock solutions of decanoate were made by dissolving solid decanoic acid in equimolar NaOH solution, followed by gentle heating and rocking. Vesicle solutions were prepared by the following steps: 1) mix solutions of salt and fluorescent dye.

2) Add decanoate solution. 3) Add liquid decanol and mix to induce vesicle assembly. The resulting vesicles encapsulated the bulk solution of salts and dyes. 4) For samples that contained glycerol-mono-decanoate, solid glycerol mono-decanoate was added to the vesicle solution, then briefly heated at 55°C to incorporate into vesicles. 5) The pH was adjusted after the amphiphiles were added. The pH adjustments were performed at room temperature, and vesicle samples were occasionally kept warm in a hot metal block.

Size-exclusion chromatography (SEC). SEC columns were prepared with 6.9 mL of Sepharose 4B resin. Before each SEC run, the column was flushed with at least two volume equivalents of running buffer. 500 μL of sample was added to the SEC column, and 400 μL fractions were

collected by hand. After all fractions were collected, the column was flushed with at least 2 volume equivalents of 0.2 M bicine (pH 9) for storage.

 $100~\mu L$  aliquots of each fraction were deposited into 96 well plates. Calcein fluorescence was measured using a Thermo Labsystems (Gulph Mills, PA) Fluoroskan Ascent FL Fluorescence Microplate Reader with ex485/em520.

For experiments using vesicle samples composed of decanoic acid and decanol (and glycerol-mono-decanoate, in some cases), the SEC running buffer contained any salts and buffers that were present in the original vesicle sample, to match ionic conditions. Regardless of the vesicle composition, the SEC running buffer contained decanoic acid at only 20 mM so that the total amphiphile concentration never dropped below the critical vesicle concentration. Higher concentrations caused the SEC resin to clog due to the large number of vesicles. Nonetheless, individual vesicles containing decanol (and glycerol-mono-decanoate, in some cases) were stable for hours after SEC despite dilution of the amphiphiles during SEC.

For samples of phospholipid vesicles, the SEC running buffer contained only salts and buffers that were present in the sample to match ionic conditions. No additional phospholipid was included in the SEC running buffer.

Fluorescence microscopy. 100 μL samples were prepared for imaging by mixing vesicle solutions with 2 mM rhodamine 6G stock (membrane dye). The rhodamine 6G concentration in final samples was between 20 μM and 40 μM. The edges of a cover slip were coated with vacuum grease and 80 μL of sample was placed in the resulting well. Another cover slip was placed on top. Images were collected on a Nikon (Melville, NY) Eclipse upright epifluorescence microscope (ME600L). A Chroma (Bellows Falls, VT) FITC/Alexa488 filter cube was used for

calcein fluorescence images (aqueous dye), and a Chroma mCherry/Texas Red filter cube was used for rhodamine fluorescence images. In the rhodamine 6G channel, vesicles appear as a bright ring when they are much larger than the objective's depth of field and when the focus is at the vesicle midplane. When vesicles are relatively small and/or they are imaged above or below the midplane, the rhodamine 6G fluorescence appears as a bright circle rather than a ring. A Wavelength Electronics (Bozeman, MT) temperature controller was used to maintain the imaging stage at desired temperature.

Experiments on flocculation with different amphiphile concentrations (Fig 2). For 60 mM amphiphile samples, vesicles were made from 40 mM decanoic acid, 10 mM decanol, 10 mM glycerol-mono-decanoate. For 300 mM amphiphile samples, vesicles were made from 200 mM decanoic acid, 50 mM decanol, 50 mM glycerol-mono-decanoate. In both cases, the solution inside and outside the vesicles contained 0.5 mM calcein and 300 mM NaHCO<sub>3</sub>. For samples with saturated NaHCO<sub>3</sub>, enough NaHCO<sub>3</sub> was added for 1.5 M if it were all soluble, but excess accumulated as solid leaving a saturated NaHCO<sub>3</sub> (~1.2 M) solution. Regardless of NaHCO<sub>3</sub> concentration, final pH was adjusted to 8.7 (± 0.05).

SEC was performed with running buffer that contained 20 mM decanoic acid and either 300 mM NaHCO<sub>3</sub> or saturated NaHCO<sub>3</sub>. In both cases, the running buffer was adjusted to pH  $8.7 (\pm 0.05)$ . The entire experiment, including imaging, was performed at  $40^{\circ}$ C.

Experiments on calcein retention during flocculation by saturated NaHCO<sub>3</sub> (Fig 3).

Vesicles were made from 100 mM decanoic acid and 50 mM decanol. The solution inside and outside the vesicles contained 5 mM calcein and 375 mM NaHCO<sub>3</sub>. pH was adjusted to 8.7 (± 0.05). Unencapsulated calcein was removed by SEC, where the running buffer contained

20 mM decanoic acid and 375 mM NaHCO<sub>3</sub> at pH 8.7 (± 0.05). SEC fractions corresponding to vesicles (early eluting) were combined, and the vesicles were mixed with a pH 8.7 (± 0.05) saturated NaHCO<sub>3</sub> solution. The final mixture was also saturated with ~1.2 M NaHCO<sub>3</sub> (enough NaHCO<sub>3</sub> was added for 1.5 M if it were all soluble, but excess accumulated as solid leaving a saturated NaHCO<sub>3</sub> solution). Vesicles were added to a saturated NaHCO<sub>3</sub> solution instead of solid NaHCO<sub>3</sub> to prevent changes to the pH upon mixing. After 1 hour, the NaHCO<sub>3</sub> was diluted to at most 375 mM in a solution of 50 mM decanoic acid and 25 mM decanol at pH 8.7 (± 0.05). Dilution into a 50 mM decanoic acid and 25 mM decanol solution prevented the amphiphile concentration from decreasing below the critical vesicle concentration. The entire experiment, including imaging, was performed at 40°C. To acquire images of vesicles, aliquots were diluted in SEC running buffer (1 vesicle aliquot: 3 SEC running buffer, by volume) to reduce the concentration of vesicles, and thus improve image quality by reducing out-of-focus light.

Experiments on calcein retention during flocculation by saturated NaCl (Fig 3). Vesicles were made from 250 mM decanoic acid and 125 mM decanol. The solution inside and outside the vesicles contained 5 mM calcein, 100 mM NaCl, and 50 mM bicine. pH was adjusted to 8.7 (± 0.05). Unencapsulated calcein was removed by SEC, where the running buffer contained 20 mM decanoic acid, 100 mM NaCl, and 50 mM bicine at pH 8.7 (± 0.05). SEC fractions corresponding to vesicles (early eluting) were combined, and solid NaCl was added to the vesicles for a saturated ~6.1 M NaCl solution (enough NaCl was added for 7.2 M if it were all soluble, but excess accumulated as solid). After 1 hour, the NaCl was diluted to at most 400 mM in a solution of 30 mM decanoic acid and 50 mM bicine at pH 8.7 (± 0.05). Dilution into a 30 mM decanoic acid and 50 mM bicine solution prevented the amphiphile concentration from decreasing below the CVC. The entire experiment, including imaging, was performed at 40°C.

To acquire images of vesicles before the addition of solid NaCl, an aliquot was diluted in SEC running buffer (1 vesicle aliquot: 3 SEC running buffer, by volume) to reduce the concentration of vesicles, and thus improve image quality by reducing out-of-focus light.

During flocculation, the encapsulated calcein became further concentrated, resulting in self-quenching (Fig S7-S8). To improve image quality by reducing self-quenching, an identical experiment was performed using an initial calcein concentration of only 0.5 mM. Images from this flocculated sample are presented in Fig 3.

Experiments on carboxyfluorescein leakage (Fig 4). Vesicles were made from 100 mM decanoic acid and 50 mM decanol. The initial solution inside and outside the vesicles contained 20 mM carboxyfluorescein and 100 mM NaHCO<sub>3</sub>. pH was adjusted to 8.7 (± 0.05). Unencapsulated carboxyfluorescein was removed by SEC, where the running buffer contained only 20 mM decanoic acid and 100 mM NaHCO<sub>3</sub> at pH 8.7 (± 0.05). SEC fractions corresponding to vesicles (early eluting) were combined.

For experiments on non-flocculated vesicles, the post-SEC sample was diluted 1:1 with additional running buffer, and then added to an empty well on a 96 well plate.

For the saturated NaCl sample, the post-SEC sample was diluted 1:1 with additional running buffer, and then added to a well that contained enough solid NaCl for a saturated ~6.1 M NaCl solution (enough NaCl was added for 7.2 M if it were all soluble, but excess accumulated as solid). Microscopy was used to confirm that the vesicles were flocculated (Fig S12).

For the saturated NaHCO<sub>3</sub> sample, the post-SEC sample was diluted 1:1 with pH 8.7 ( $\pm$  0.05) saturated NaHCO<sub>3</sub> solution inside of a well on a 96 well plate. The final mixture was

also saturated with ~1.2 M NaHCO<sub>3</sub> (enough NaHCO<sub>3</sub> was added for 1.8 M if it were all soluble, but excess accumulated as solid leaving a saturated NaHCO<sub>3</sub> solution). Vesicles were added to a saturated NaHCO<sub>3</sub> solution instead of solid NaHCO<sub>3</sub> to prevent changes to the pH upon mixing. Microscopy was used to confirm that the vesicles were flocculated (Fig S12).

In all cases, duplicate 100  $\mu$ L aliquots were placed in 96 well plates, and carboxyfluorescein fluorescence (ex485/em520) was measured in triplicate. The same two duplicate aliquots were measured at each time point.

In parallel duplicate aliquots, Triton-X-100 was added (t=0) to induce complete disruption of encapsulation by vesicles or flocs. Enough Triton-X-100 was added for 0.32% (mass/mass), but addition of Triton-X-100 only changed the sample volume by 2%.

Carboxyfluorescein fluorescence was measured every 0.5 hr. The 96 well plate was shaken before each measurement to evenly distribute the flocs across the well. For the samples without initial Triton-X-100, Triton-X-100 was added after the final timepoint, and fluorescence measured again.

Experiments on calcein retention during dehydration (Fig 5). Vesicles were made from 100 mM decanoic acid, 25 mM decanol, and 25 mM glycerol-mono-decanoate. The initial solution inside and outside the vesicles contained 5 mM calcein, 100 mM NaCl, and 50 mM bicine. pH was adjusted to 8.7 ( $\pm$  0.05). The SEC running buffer contained only 20 mM decanoic acid, 100 mM NaCl, and 50 mM bicine at pH 8.7 ( $\pm$  0.05).

For experiments on phospholipid vesicles, a film composed of 5 mg 95% DOPC and 5% DOPG was hydrated for about 72 hours with 1 mL of 5 mM calcein, 100 mM NaCl, and 50 mM

bicine solution at pH 8.7 ( $\pm$  0.05). After 72 hours of hydration, the vesicle solution was again adjusted to pH 8.7 ( $\pm$  0.05). The SEC running buffer contained only 100 mM NaCl and 50 mM bicine at pH 8.7 ( $\pm$  0.05).

During experiments on either fatty acid vesicles or phospholipid vesicles, unencapsulated calcein was removed by SEC, and fractions corresponding to vesicles (early eluting) were combined. 200  $\mu$ L aliquots of the combined fractions were distributed to separate test tubes, and each tube was dried at room temperature under a stream of  $N_2$  for 1 hour. Next, the mass of each test tube and sample was measured, and the test tubes were again put under a stream of  $N_2$  for an additional 0.5 hour. Final mass measurements of each test tube and sample confirmed that there were no detectable changes in mass (within  $\pm$  0.5 mg), so the samples were deemed dehydrated. The dry samples were immediately rehydrated with 200  $\mu$ L H2O, allowed to sit at room temperature for 1 hour, then vortexed vigorously to resolubilize dried material.

#### **RESULTS AND DISCUSSION:**

Vesicles flocculated in saturated salt solution, independent of whether they were made of fatty acids or phospholipids. For example, vesicles of 4:1:1 DA:DOH:GMD flocculated in saturated NaHCO<sub>3</sub>, independent of the fatty acid concentration (Fig 2). Even when the concentration of amphiphile was increased (as would occur during dehydration), vesicles still flocculated when the NaHCO<sub>3</sub> became saturated (Fig 2e). No vesicles escaped flocculation, independent of whether the sample was evaluated by fluorescence microscopy or by size-exclusion chromatography (SEC). The composition 4:1:1 DA:DOH:GMD was chosen because

those vesicles are more stable than vesicles of 2:1 DA:DOH<sup>28</sup>. Phospholipid vesicles of 95:5 DOPC:DOPG flocculated under the same salt conditions (Fig S1-S2).

Our central question is whether flocculation disrupts encapsulation of solutes by fatty acid vesicles. We prepared vesicles of 2:1 DA:DOH encapsulating calcein dye as a proxy for prebiotic molecules (Fig 3). We found that the dye remained in the vesicle lumens throughout a two-step cycle of flocculation in high salt and dispersal in low salt. This result held independent of whether flocculation was achieved with saturated NaHCO<sub>3</sub> or with saturated NaCl.

Surprisingly in light of previous work, glycerol-mono-decanoate was not required for membrane stability<sup>11</sup>. Because calcein is a relatively small molecule, we can be confident that flocculated vesicles are also impermeable to larger molecules like ribozymes.

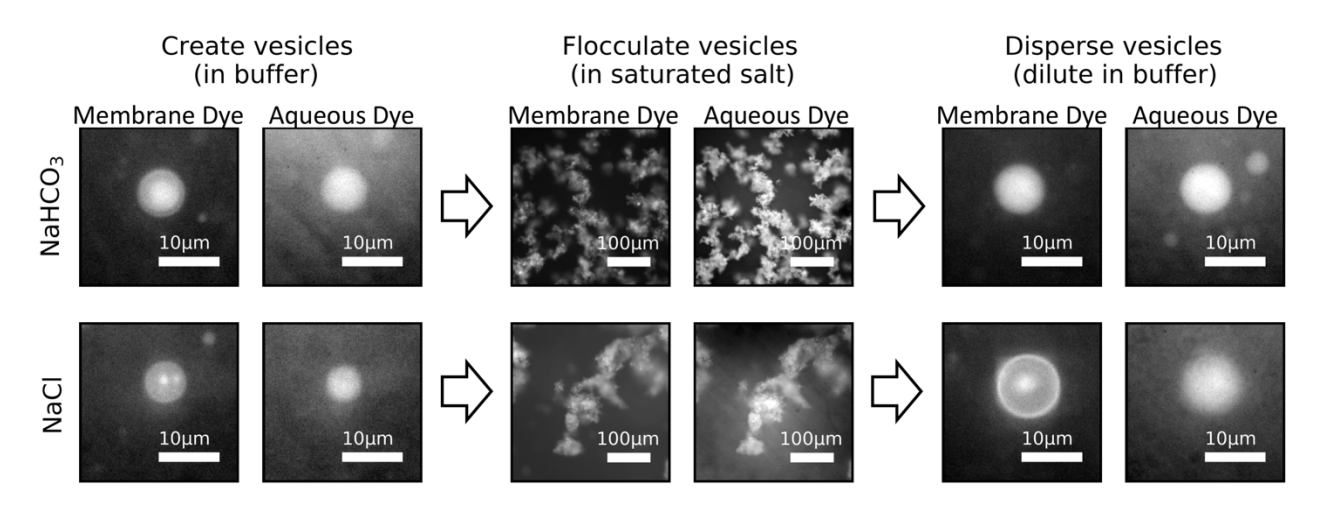


**Figure 3.** Fatty acid vesicles composed of 2:1 DA:DOH maintained encapsulation of an aqueous dye (calcein) throughout a process of salt-induced flocculation and subsequent dispersal. Immediately after adding salt, the vesicles flocculated; after 1 hr, the salt was diluted. Encapsulation was maintained independent of which saturated salt (~1.2 M NaHCO<sub>3</sub> or ~6.1 M NaCl) was used to induce flocculation. The dye that labeled vesicle membranes (rhodamine 6G) was added immediately prior to imaging. To optimize imaging (which did not change the results), we varied the preparation or treatment of samples in two ways. First, the samples shown in the left columns (the initial vesicles) and at the top right (after dilution from saturated NaHCO<sub>3</sub>) were diluted 1:3 with SEC running buffer prior to imaging. Second, in the bottom row, flocculated vesicles in NaCl encapsulated a low (0.5 mM) initial calcein concentration to prevent self-quenching, whereas vesicles before and after flocculation encapsulated 5 mM calcein

initially. More discussion of this issue, and corresponding wide-field images are in the SI (Fig S3-S9).

In addition to our qualitative results from imaging, we verified quantitatively that the rate of dye leakage is not faster from flocculated vesicles than from dispersed vesicles (Fig 4). We encapsulated a self-quenching concentration of carboxyfluorescein in vesicles; an increase in fluorescence indicated leakage into the surrounding solution. We flocculated the vesicles with saturated NaHCO<sub>3</sub> or saturated NaCl. We did not observe leakage of the dye on the timescale (~ 3 h) of the experiment. As a positive control, we artificially achieved total leakage by disrupting the vesicles with Triton-X-100. We used microscopy to confirm that vesicles flocculated in these saturated salt conditions (Fig S12).

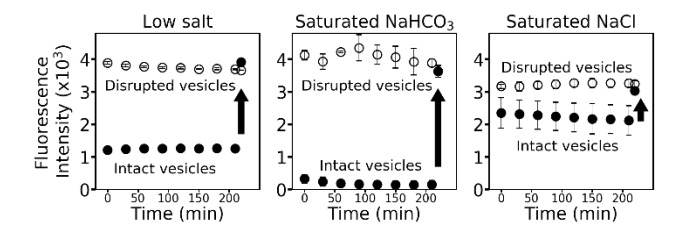


**Figure 4.** Single vesicles (low salt: 100mM NaHCO<sub>3</sub>) and flocculated vesicles (saturated salt) encapsulated a dye on long time scales (>3 hours). Vesicles composed of 2:1 DA:DOH were formed in a solution with a self-quenching concentration (20 mM) of carboxyfluorescein dye. Unencapsulated dye was removed by SEC. Fluorescence intensity increased when the dye leaked out of vesicles and decreased when the dye photobleached. At each time point, the same two aliquots were assayed. In one, vesicles were intact (filled symbols). In the other, vesicles were disrupted with Triton-X-100, leading to total release of the dye (open symbols). At the last timepoint, the intact vesicles were also disrupted with Triton-X-100 (arrows). Triton-X-100 did not affect the fluorescence (Fig S10). We observed that carboxyfluorescein fluorescence varies with the type and concentration of salt (Fig S10-S11); calcein fluorescence is also known to be quenched by some divalent cations<sup>29</sup>. Error bars are standard deviations of two independent experiments. When error bars are not shown, they are smaller than the symbols.

The challenge of predicting whether flocculation of membranes will lead to leakage of vesicle contents underscores the importance of our measurements. Flocculation of vesicles will result in vesicle rupture if adhesion between vesicles generates tensions that exceed the lysis tension (~ 5-10 mN/m for phospholipid membranes)<sup>30</sup>. Tension also favors the formation of pores in membranes<sup>31</sup>, which can lead to loss of vesicle contents. Previous work focused on vesicles of phospholipids, and showed that they remain intact during salt-induced flocculation<sup>32</sup>. Compared to phospholipid membranes, fatty acid membranes might be expected to have higher densities of hydrophobic defects, which are a precursor to pore formation<sup>31</sup>. However, it is difficult to predict whether fatty acid membranes are uniformly more susceptible to pore formation than phospholipid membranes because the packing of fatty acids is sensitive to their charge, which may be different at the membrane surface than in solution<sup>33</sup>. Pore formation in a single membrane is stabilized when each leaflet of the membrane has a positive spontaneous curvature<sup>31</sup>, as expected for fatty acid membranes near a micelle transition. On the other hand, at low pH, the addition of fatty acids to phospholipid membranes imparts a negative spontaneous curvature and a high bending rigidity<sup>34</sup>.

Our results above imply that fatty acid-based protocells could have survived salt-induced flocculation during an evaporative cycle, but what if the evaporation were complete? We found that fatty acid vesicles lost the ability to encapsulate calcein dye within 30 min of dehydration, even when glycerol-mono-decanoate was incorporated to provide additional stability (4:1:1 DA:DOH:GMD) (Fig 5). After rehydration, dried fatty acids reassembled into vesicles, and the encapsulated solution had a similar dye concentration to the exterior solution. After the dye was removed from the exterior solution by SEC, the encapsulated solution again appeared brighter (Fig S16). Our observations with decanoic acid vesicles are consistent with a report that only about 1% of encapsulated calcein is retained during dehydration of oleic acid vesicles<sup>35</sup> (although oleic

acid is unlikely to have been present on the prebiotic Earth because natural abiotic synthesis has not been observed). The presence of sugars in the prebiotic environment could have improved retention upon formation of a glassy precipitate<sup>36</sup>.

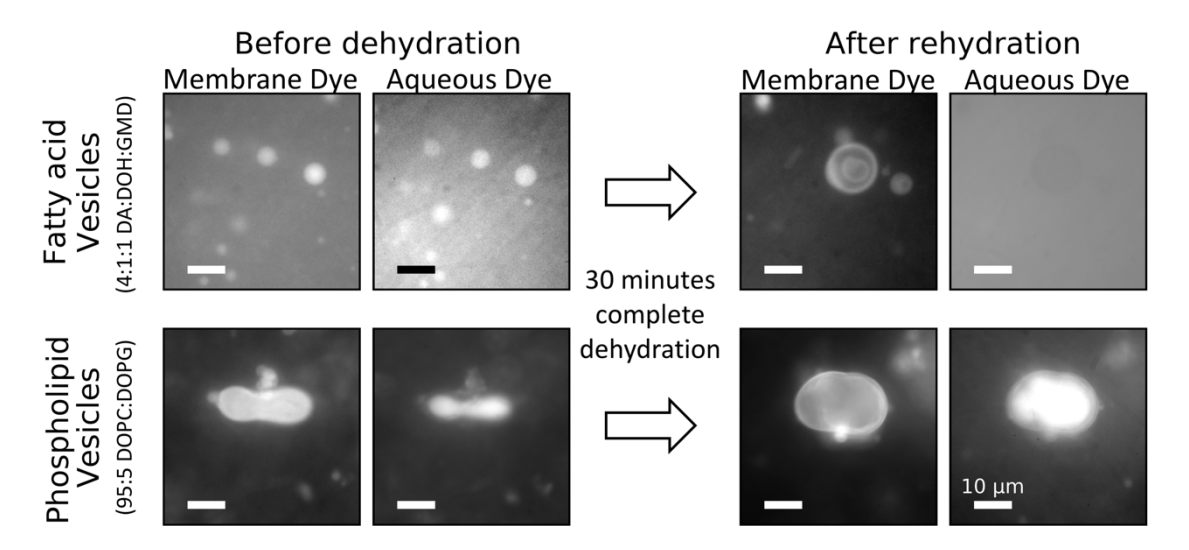


**Figure 5.** Vesicles of fatty acids (4:1:1 DA:DOH:GMD, top) and phospholipids (95:5 DOPC:DOPG, bottom) initially encapsulated an aqueous dye (calcein). After 30 minutes of dehydration and 60 minutes of rehydration, fatty acid vesicles were visible with a mem-brane dye, but they no longer encapsulated the aqueous dye (top right micrograph). In contrast, after the same dehydration cycle, phospholipid vesicles still encapsulated the aqueous dye (bottom right micrograph). In all samples, the dye that labeled vesicle membranes (rhodamine 6G) was added immediately prior to imaging. Corresponding wide-field images are in the SI (Fig S13-S19). Scale bars are 10 μm.

In contrast to fatty acid vesicles, phospholipid vesicles retained encapsulated calcein after 30 min of dehydration and rehydration (Fig 5). Based on previous studies, the amount of retained dye may decrease as dry periods become longer<sup>37</sup>. The ability of dried phospholipid vesicles to reencapsulate the bulk solution during rehydration had previously been demonstrated<sup>38</sup>. Before the emergence of phospholipids, cycles of dehydration and rehydration would have induced mixing between protocells, which may have been a primitive mechanism for exchanging genetic material. Incorporation of phospholipids could have provided an advantage to individual protocells by preserving their encapsulated contents.

#### CONCLUSION:

When vesicles of fatty acids flocculate in saturated solutions of monovalent salts, they maintain encapsulation of dye molecules as well as dispersed vesicles do. In contrast, prebiotically plausible coacervates are disrupted in relatively dilute NaCl solutions (250 mM), although they can reassemble after complete dehydration and rehydration to sequester charged polymers<sup>39</sup>. Within dynamic lake environments that experience dehydration and rehydration on diurnal or seasonal timescales<sup>40</sup>, fatty acid-based vesicles may have grown and divided during periods when the salt concentration was low, and then retained their contents despite flocculation during periods of high salt concentration.

While fatty acid vesicles do not retain encapsulated material through periods of complete dehydration, we show that phospholipid vesicles can. Taken together, our results are consistent with the hypothesis that evaporating pools on Earth's surface were conducive to protocell development, and not an obstacle as previously thought.

#### ASSOCIATED CONTENT:

**Supporting Information**. Additional images and data. This material is available free of charge via the Internet at http://pubs.acs.org."

#### **AUTHOR INFORMATION:**

#### **Corresponding Author**

\* To whom correspondence may be addressed. Email: zrcohen2@uw.edu, dcatling@uw.edu, or slkeller@uw.edu.

#### **Present Addresses**

† Department of Bioengineering, University of California Berkeley, Berkeley, CA, USA.

#### **Author Contributions**

Z.R.C. and C.E.C. conducted experiments. Z.R.C, R.A.B, D.C.C, and S.L.K. analyzed data.

Z.R.C, R.A.B, D.C.C, and S.L.K. wrote the manuscript. All authors have given approval to the final version of the manuscript.

#### ACKNOWLEDGMENT:

This work was supported in part by a grant (NNX17AK86G, Exobiology) from NASA to S.L.K. and R.A.B, by a grant (MCB 1925731) from the NSF to S.L.K, and by a grant (511570FY20, DCC) from the Simons Foundation to D.C.C. ZRC was funded by an NSF fellowship (NSF GRFP DGE 1762114). We thank Dr. Zoe Todd for guidance with vesicle experiments.

#### ABBREVIATIONS:

DA, decanoic acid; DOH, decanol; GMD, glycerol-mono-decanoate; NaHCO<sub>3</sub>, sodium bicarbonate; NaCl, sodium chloride; SEC, size-exclusion chromatography; DOPC, 1,2-dioleoyl-sn-glycero-3-phosphocholine; DOPG, 1,2-dioleoyl-sn-glycero-3-phospho-(1'-rac-glycerol).

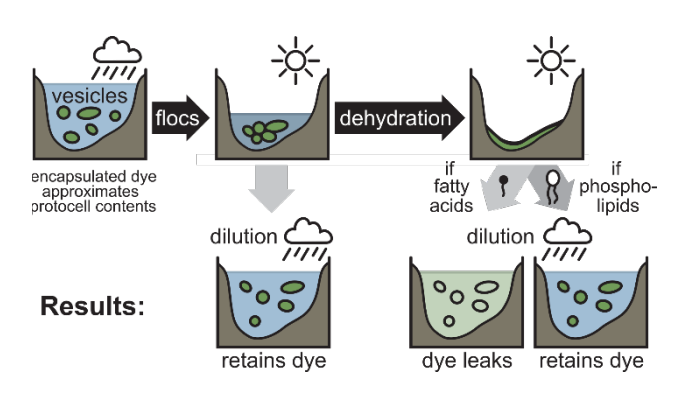
#### REFERENCES:

- (1) Deamer, D.; Dworkin, J. P.; Sandford, S. A.; Bernstein, M. P.; Allamandola, L. J. The First Cell Membranes. *Astrobiology* **2002**, *2* (4), 371–381.
- (2) Lawless, J. G.; Yuen, G. U. Quantification of Monocarboxylic Acids in the Murchison Carbonaceous Meteorite. *Nature* **1979**, *282* (5737), 396–398.
- (3) Nooner, D. W.; Oro, J. Synthesis of Fatty Acids by a Closed System Fischer-Tropsch Process. In *Hydrocarbon Synthesis from Carbon Monoxide and Hydrogen*; Advances in Chemistry; American Chemical Society, **1979**; Vol. 178, pp 159–171.
- (4) Yuen, G. U.; Lawless, J. G.; Edelson, E. H. Quantification of Monocarboxylic Acids from a Spark Discharge Synthesis. *J Mol Evol* **1981**, *17* (1), 43–47.
- (5) Black, R. A.; Blosser, M. C. A Self-Assembled Aggregate Composed of a Fatty Acid Membrane and the Building Blocks of Biological Polymers Provides a First Step in the Emergence of Protocells. *Life* **2016**, *6* (3), 33.
- (6) Joyce, G. F.; Szostak, J. W. Protocells and RNA Self-Replication. *Cold Spring Harb Perspect Biol* **2018**, *10* (9), a034801.
- (7) Lopez, A.; Fiore, M. Investigating Prebiotic Protocells for a Comprehensive Understanding of the Origins of Life: A Prebiotic Systems Chemistry Perspective. *Life* **2019**, *9* (2), 49.
- (8) Apel, C. L.; Deamer, D. W.; Mautner, M. N. Self-Assembled Vesicles of Monocarboxylic Acids and Alcohols: Conditions for Stability and for the Encapsulation of Biopolymers. *Biochimica et Biophysica Acta (BBA) Biomembranes* **2002**, *1559* (1), 1–9.
- (9) Maurer, S. E.; Nguyen, G. Prebiotic Vesicle Formation and the Necessity of Salts. *Orig Life Evol Biosph* **2016**, *46* (2–3), 215–222.
- (10) Weitz, D. A.; Lin, M. Y.; Lindsay, H. M. Universality Laws in Coagulation. *Chemometrics and Intelligent Laboratory Systems* **1991**, *10* (1), 133–140.
- (11) Monnard, P.-A.; Apel, C. L.; Kanavarioti, A.; Deamer, D. W. Influence of Ionic Inorganic Solutes on Self-Assembly and Polymerization Processes Related to Early Forms of Life: Implications for a Prebiotic Aqueous Medium. *Astrobiology* **2002**, *2* (2), 139–152.
- (12) Rosing, M. T. 13C-Depleted Carbon Microparticles in >3700-Ma Sea-Floor Sedimentary Rocks from West Greenland. *Science* **1999**, *283* (5402), 674–676.
- (13) Ohtomo, Y.; Kakegawa, T.; Ishida, A.; Nagase, T.; Rosing, M. T. Evidence for Biogenic Graphite in Early Archaean Isua Metasedimentary Rocks. *Nature Geosci* **2014**, *7* (1), 25–28.
- (14) Korenaga, J. Was There Land on the Early Earth? *Life* **2021**, *11* (11), 1142.
- (15) Tang, M.; Chen, K.; Rudnick, R. L. Archean Upper Crust Transition from Mafic to Felsic Marks the Onset of Plate Tectonics. *Science* **2016**, *351* (6271), 372–375.
- (16) Eugster, H. P.; Jones, B. F. Behavior of Major Solutes during Closed-Basin Brine Evolution. *American Journal of Science* **1979**, *279* (6), 609–631.
- (17) Sasselov, D. D.; Grotzinger, J. P.; Sutherland, J. D. The Origin of Life as a Planetary Phenomenon. *Science Advances* **2020**, *6* (6), eaax3419.
- (18) Damer, B.; Deamer, D. The Hot Spring Hypothesis for an Origin of Life. *Astrobiology* **2019**, 20 (4), 429–452.
- (19) Toner, J. D.; Catling, D. C. Alkaline Lake Settings for Concentrated Prebiotic Cyanide and the Origin of Life. *Geochimica et Cosmochimica Acta* **2019**, *260*, 124–132.
- (20) Toner, J. D.; Catling, D. C. A Carbonate-Rich Lake Solution to the Phosphate Problem of the Origin of Life. *Proc Natl Acad Sci USA* **2020**, *117* (2), 883–888.

- (21) Patel, B. H.; Percivalle, C.; Ritson, D. J.; Duffy, C. D.; Sutherland, J. D. Common Origins of RNA, Protein and Lipid Precursors in a Cyanosulfidic Protometabolism. *Nature Chemistry* **2015**, *7* (4), 301–307.
- (22) Rodriguez-Garcia, M.; Surman, A. J.; Cooper, G. J. T.; Suárez-Marina, I.; Hosni, Z.; Lee, M. P.; Cronin, L. Formation of Oligopeptides in High Yield under Simple Programmable Conditions. *Nat Commun* 2015, 6 (1), 8385.
- (23) Forsythe, J. G.; Yu, S.-S.; Mamajanov, I.; Grover, M. A.; Krishnamurthy, R.; Fernández, F. M.; Hud, N. V. Ester-Mediated Amide Bond Formation Driven by Wet–Dry Cycles: A Possible Path to Polypeptides on the Prebiotic Earth. *Angewandte Chemie International Edition* 2015, 54 (34), 9871–9875.
- (24) Black, R. A.; Blosser, M. C.; Stottrup, B. L.; Tavakley, R.; Deamer, D. W.; Keller, S. L. Nucleobases Bind to and Stabilize Aggregates of a Prebiotic Amphiphile, Providing a Viable Mechanism for the Emergence of Protocells. *Proceedings of the National Academy of Sciences* **2013**, *110* (33), 13272–13276.
- (25) Cornell, C. E.; Black, R. A.; Xue, M.; Litz, H. E.; Ramsay, A.; Gordon, M.; Mileant, A.; Cohen, Z. R.; Williams, J. A.; Lee, K. K.; Drobny, G. P.; Keller, S. L. Prebiotic Amino Acids Bind to and Stabilize Prebiotic Fatty Acid Membranes. *Proc Natl Acad Sci USA* **2019**, *116* (35), 17239–17244.
- (26) Zorz, J. K.; Sharp, C.; Kleiner, M.; Gordon, P. M. K.; Pon, R. T.; Dong, X.; Strous, M. A Shared Core Microbiome in Soda Lakes Separated by Large Distances. *Nat Commun* **2019**, *10* (1), 4230.
- (27) Mansy, S. S.; Schrum, J. P.; Krishnamurthy, M.; Tobé, S.; Treco, D. A.; Szostak, J. W. Template-Directed Synthesis of a Genetic Polymer in a Model Protocell. *Nature* **2008**, *454* (7200), 122–125.
- (28) Mansy, S. S.; Szostak, J. W. Thermostability of Model Protocell Membranes. *Proc Natl Acad Sci U S A* **2008**, *105* (36), 13351–13355.
- (29) Breuer, W.; Epsztejn, S.; Millgram, P.; Cabantchik, I. Z. Transport of Iron and Other Transition Metals into Cells as Revealed by a Fluorescent Probe. *American Journal of Physiology-Cell Physiology* **1995**, *268* (6), C1354–C1361.
- (30) Evans, E. A. Analysis of Adhesion of Large Vesicles to Surfaces. *Biophysical Journal* **1980**, 31 (3), 425–431.
- (31) Akimov, S. A.; Volynsky, P. E.; Galimzyanov, T. R.; Kuzmin, P. I.; Pavlov, K. V.; Batishchev, O. V. Pore Formation in Lipid Membrane I: Continuous Reversible Trajectory from Intact Bilayer through Hydrophobic Defect to Transversal Pore. *Sci Rep* **2017**, *7* (1), 12152.
- (32) Pigor, T.; Lawaczeck, R. On the Interaction of Phospholipid Vesicles with Chaotropic Ions. *Z. Naturforsch* **1983**, *38* (3–4), 307–312.
- (33) Gilbile, D.; Docto, D.; Kingi, D. T.; Kurniawan, J.; Monahan, D.; Tang, A.; Kuhl, T. L. How Well Can You Tailor the Charge of Lipid Vesicles? *Langmuir* **2019**, *35* (48), 15960–15969.
- (34) Tyler, A. I. I.; Greenfield, J. L.; Seddon, J. M.; Brooks, N. J.; Purushothaman, S. Coupling Phase Behavior of Fatty Acid Containing Membranes to Membrane Bio-Mechanics. *Frontiers in Cell and Developmental Biology* **2019**, *7*, 187.
- (35) Sarkar, S.; Dagar, S.; Rajamani, S. Influence of Wet–Dry Cycling on the Self-Assembly and Physicochemical Properties of Model Protocellular Membrane Systems. *ChemSystemsChem* **2021**, *3* (5), e2100014.

- (36) Sun, W. Q.; Leopold, A. C.; Crowe, L. M.; Crowe, J. H. Stability of Dry Liposomes in Sugar Glasses. *Biophysical Journal* **1996**, *70* (4), 1769–1776.
- (37) Wolkers, W. F.; Oldenhof, H.; Tablin, F.; Crowe, J. H. Preservation of Dried Liposomes in the Presence of Sugar and Phosphate. *Biochimica et Biophysica Acta (BBA) Biomembranes* **2004**, *1661* (2), 125–134.
- (38) Deamer, D. W.; Barchfeld, G. L. Encapsulation of Macromolecules by Lipid Vesicles under Simulated Prebiotic Conditions. *J Mol Evol* **1982**, *18* (3), 203–206.
- (39) Fares, H. M.; Marras, A. E.; Ting, J. M.; Tirrell, M. V.; Keating, C. D. Impact of Wet-Dry Cycling on the Phase Behavior and Compartmentalization Properties of Complex Coacervates. *Nat Commun* **2020**, *11* (1), 5423.
- (40) Yechieli, Y.; Wood, W. W. Hydrogeologic Processes in Saline Systems: Playas, Sabkhas, and Saline Lakes. *Earth-Science Reviews* **2002**, *58* (3), 343–365.

#### TABLE OF CONTENTS GRAPHIC:



# **Supporting Information:**

# Prebiotic protocell membranes retain encapsulated contents during flocculation, and phospholipids preserve encapsulation during dehydration

Zachary R. Cohen<sup>1‡\*</sup>, Caitlin. E. Cornell<sup>1†</sup>, David C. Catling<sup>2‡\*</sup>,

Roy A. Black<sup>1</sup>, Sarah L. Keller<sup>1‡\*</sup>.

### **Table of Contents**

Section 1: Phospholipid vesicles flocculate in saturated NaHCO<sub>3</sub>

Section 2: Additional images from flocculation experiments

Section 3: Additional images and data from carboxyfluorescein leakage experiments

Section 4: Additional images from dehydration experiments

<sup>&</sup>lt;sup>1</sup>Department of Chemistry, University of Washington, Seattle WA 98195, USA.

<sup>&</sup>lt;sup>2</sup>Department of Earth and Space Sciences, University of Washington, Seattle WA 98195, USA.

<sup>&</sup>lt;sup>‡</sup>Astrobiology Program, University of Washington, Seattle WA 98195, USA.

# Section 1: Phospholipid vesicles flocculate in saturated NaHCO<sub>3</sub>

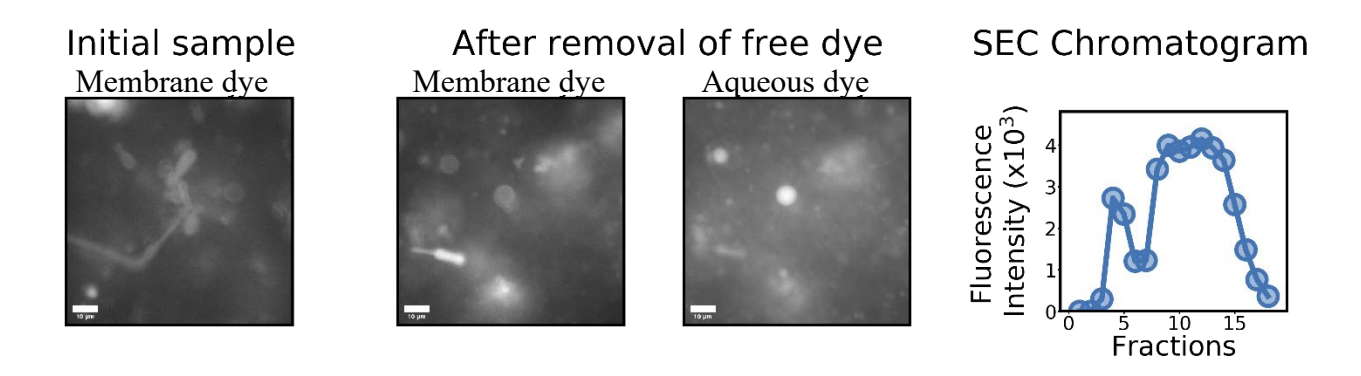


Figure S1: Phospholipid vesicles composed of 5 mg/mL 95 mol % DOPC + 5 mol % DOPG do not flocculate in the presence of 100 mM NaHCO3. Vesicles were formed by hydrating a lipid film with 5 mM calcein and 100 mM NaHCO3 for 48 hours. After 48 hours, the pH of the vesicle sample was adjusted to 8.7 ( $\pm$  0.05), and size-exclusion chromatography was performed using a running buffer consisting of 100 mM NaHCO3 at pH 8.7. Fluorescence micrographs show unaggregated vesicles before and after size-exclusion chromatography. The SEC chromatogram shows two peaks, which suggests a population of calcein-containing vesicles, in addition to unencapsulated calcein. Scale bars are 10  $\mu m$ .

### Initial sample



SEC Chromatogram

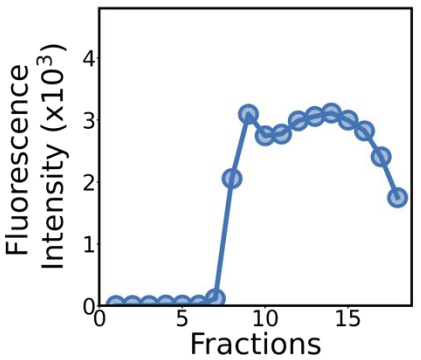


Figure S2: Phospholipid vesicles composed of 5 mg/mL 95 mol % DOPC + 5 mol % DOPG flocculate in the presence of saturated NaHCO3. Vesicles were formed by hydrating a lipid film with 5 mM calcein and 100 mM NaHCO<sub>3</sub> for 48 hours. After 48 hours, enough NaHCO3 was added for 1.8 M if it were all soluble, but excess accumulated as solid leaving a saturated ~1.2 M NaHCO<sub>3</sub> solution. The pH of the saturated solution was adjusted to 8.7 (± .05), and size-exclusion chromatography was performed using a running buffer consisting of saturated ~1.2 M NaHCO3 (enough NaHCO3 for 1.5 M if it were all soluble, but excess accumulated as solid) at pH 8.7. The fluorescence micrograph shows flocculated vesicles before size-exclusion chromatography. In the test tube, a floc layer floats above the unencapsulated calcein. At the very bottom of the test tube, a layer of undissolved NaHCO<sub>3</sub> is visible. Because the flocs are less dense than the surrounding solution, they do not flow into the SEC resin. The SEC chromatogram does not show an early-eluting peak, which suggests there are no unaggregated vesicles. Only a late eluting peak is seen in the chromatogram, corresponding to unencapsulated calcein. Scale bar is 10 µm.

# Section 2: Additional images from flocculation experiments.

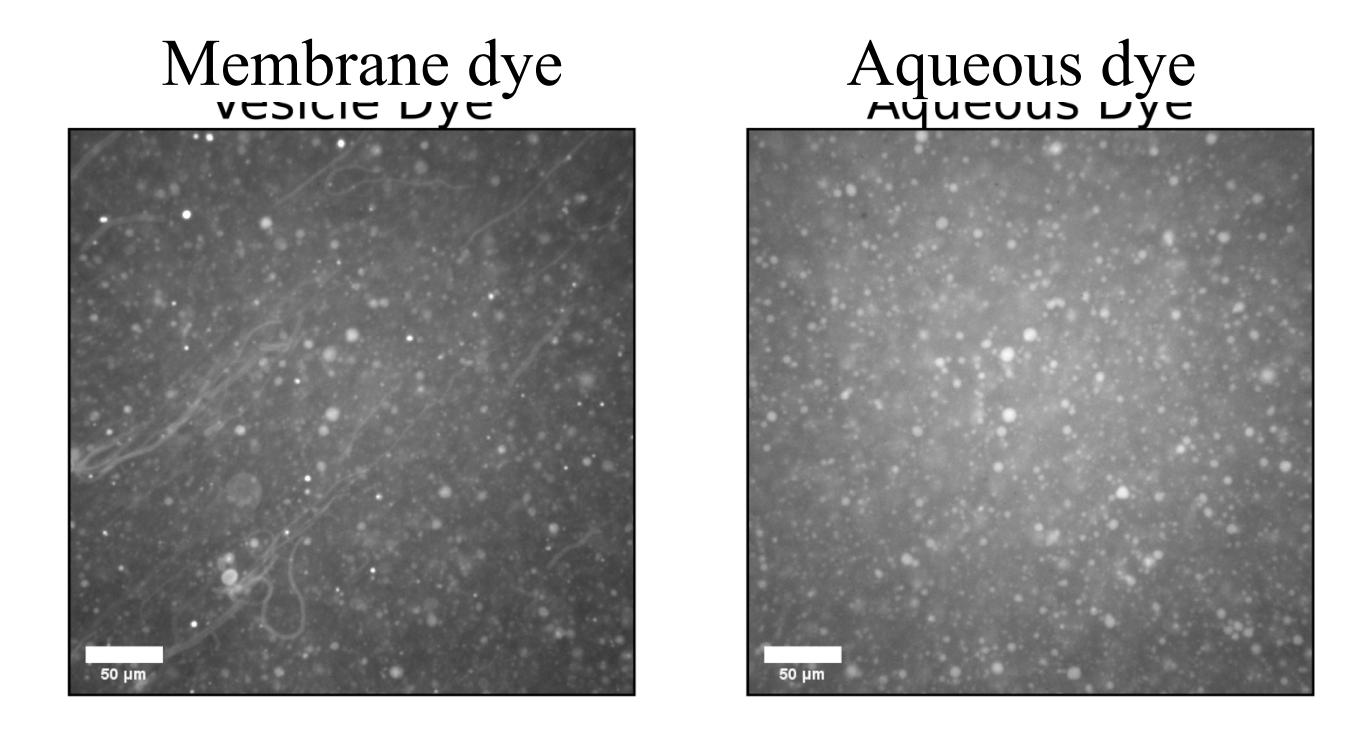


Figure S3: Additional images from the NaHCO<sub>3</sub> flocculation experiment shown in Fig 3 ("Create vesicles"). See "Experiments on calcein retention during flocculation by saturated NaHCO<sub>3</sub>" in the methods section for full details. The vesicles were diluted 1:3 with SEC running buffer prior to imaging. Scale bars are 50 μm.

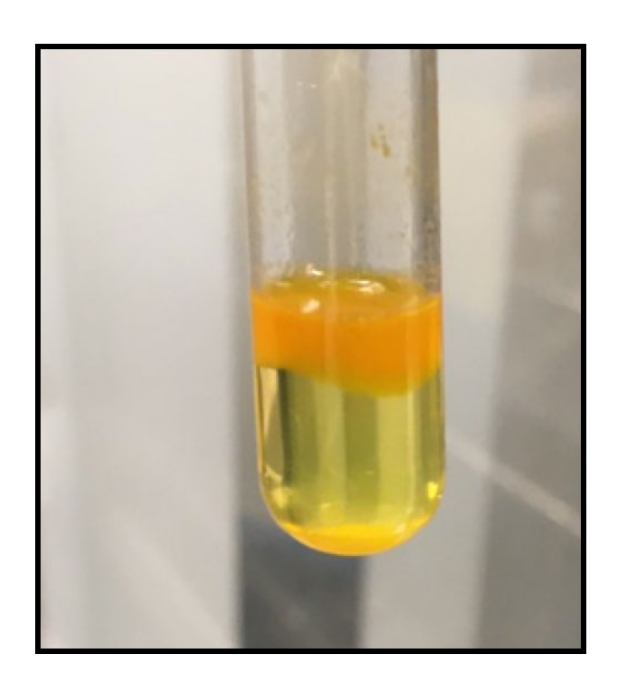
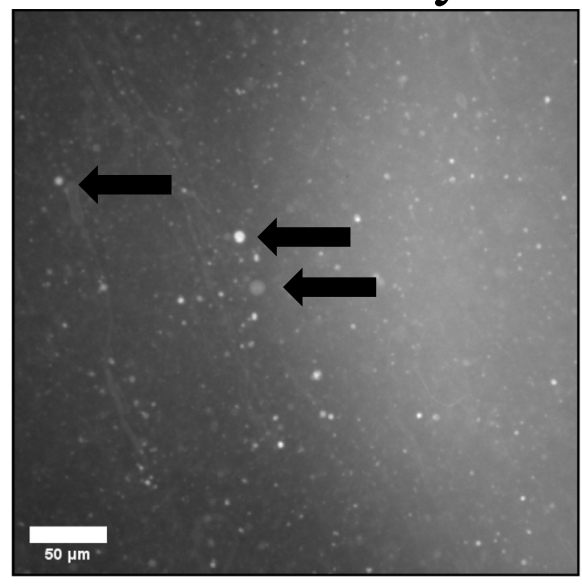


Figure S4: Additional image from the NaHCO<sub>3</sub> flocculation experiment shown in Fig 3 ("Flocculate vesicles"). Upon exposing the vesicles to saturated NaHCO<sub>3</sub>, a thick layer of flocculated vesicles can be seen in the test tube. Importantly, this floc layer is still bright with calcein. Below the low-density floc layer is a layer of solution containing unencapsulated calcein, and at the very bottom of the tube is a layer of undissolved NaHCO<sub>3</sub>. See "Experiments on calcein retention during flocculation by saturated NaHCO<sub>3</sub>" in the methods section for full details.



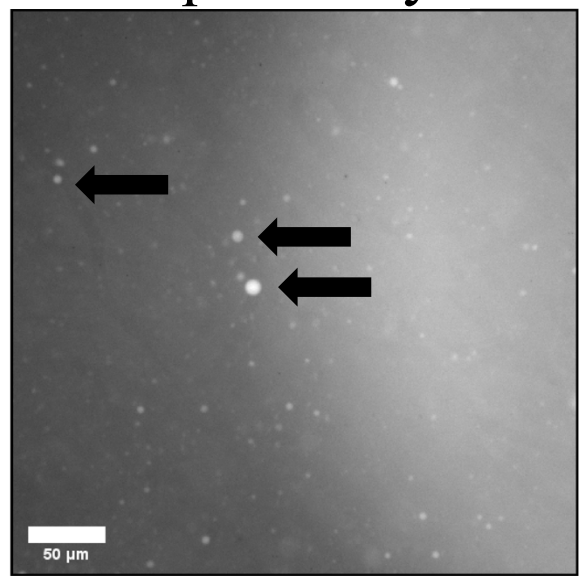
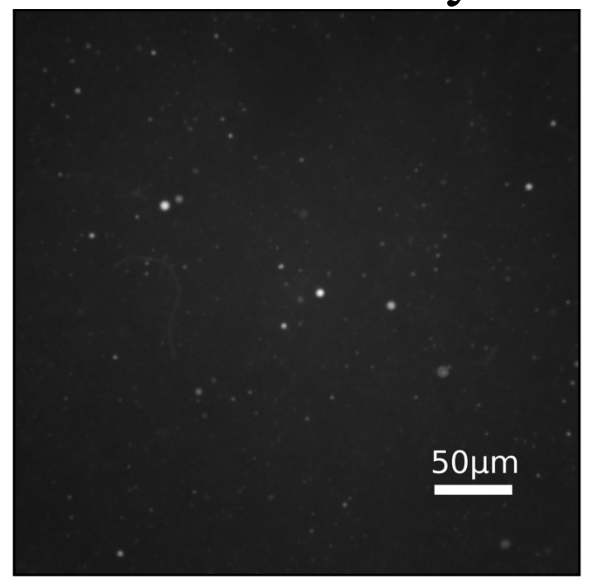


Figure S5: Additional images from the NaHCO $_3$  flocculation experiment shown in Fig 3 ("Disperse vesicles"). See "Experiments on calcein retention during flocculation by saturated NaHCO $_3$ " in the methods section for full details. The vesicles were diluted 1:3 with SEC running buffer prior to imaging. Arrows indicate a few of the vesicles that have encapsulated calcein (bright in both membrane dye and aqueous dye). Scale bars are 50  $\mu$ m.



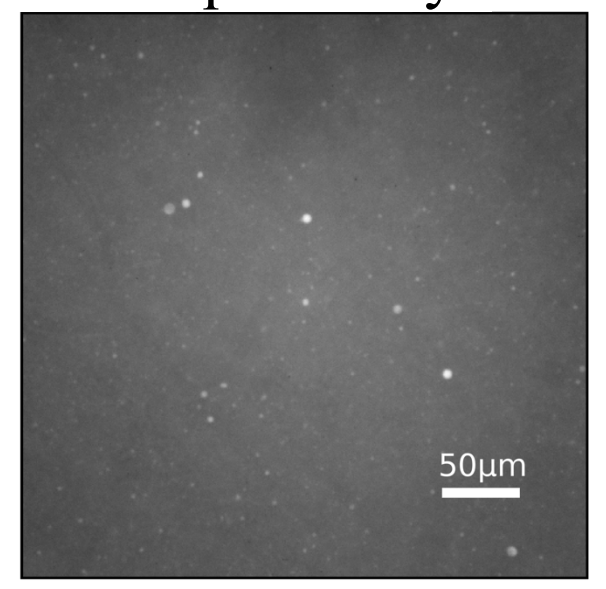
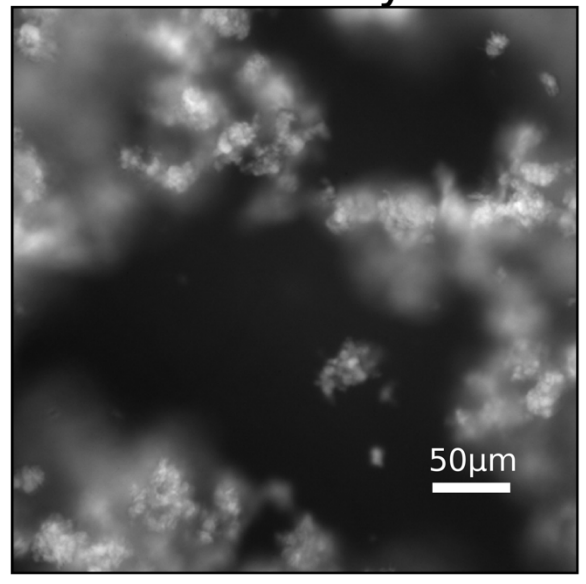


Figure S6: Additional images from the NaCl flocculation experiment shown in Fig 3 ("Create vesicles"). See "Experiments on calcein retention during flocculation by saturated NaCl" in the methods section for full details. The vesicles were diluted 1:3 with SEC running buffer prior to imaging. Scale bars are  $50 \mu m$ .



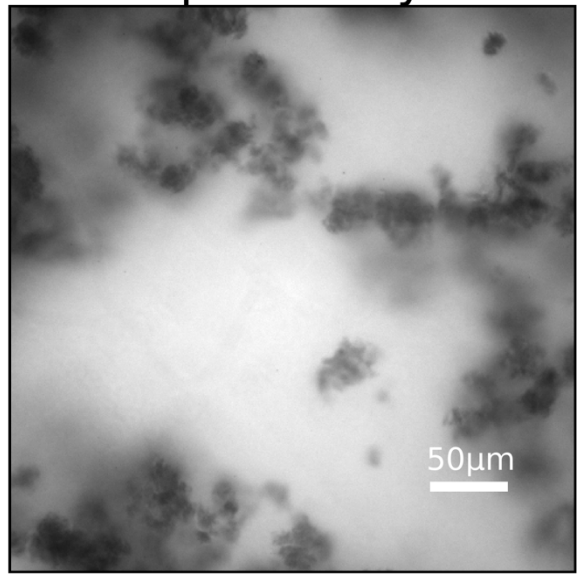


Figure S7: Alternative image from the NaCl flocculation experiment shown in Fig 3 ("Flocculate vesicles"). Unlike the image shown in Fig 3 where 0.5 mM calcein is encapsulated in flocculated vesicles, in this image the flocculated vesicles encapsulate 5 mM calcein. Upon inducing flocculation, the effective concentration of encapsulated calcein increases high enough to induce self-quenching. As a result, flocculated vesicles appear darker than the surrounding solution in the calcein channel. Prior to flocculation, this same sample is shown in Fig 3 "Create vesicles". When this sample is diluted so that the NaCl concentration is low enough to allow flocculated vesicles to disaggregate, the vesicles also appear to be bright with calcein (Fig 3 "Disperse vesicles"). See "Experiments on calcein retention during flocculation by saturated NaCl" in the methods section for full details. Scale bars are 50  $\mu$ m.

# 5mM calcein



# 0.5mM calcein

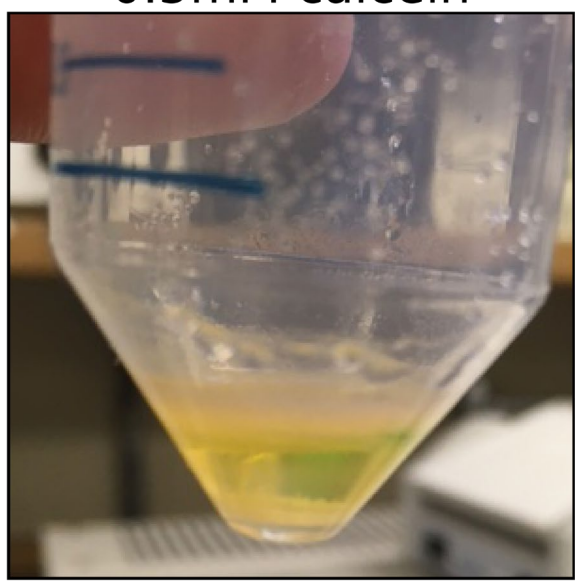
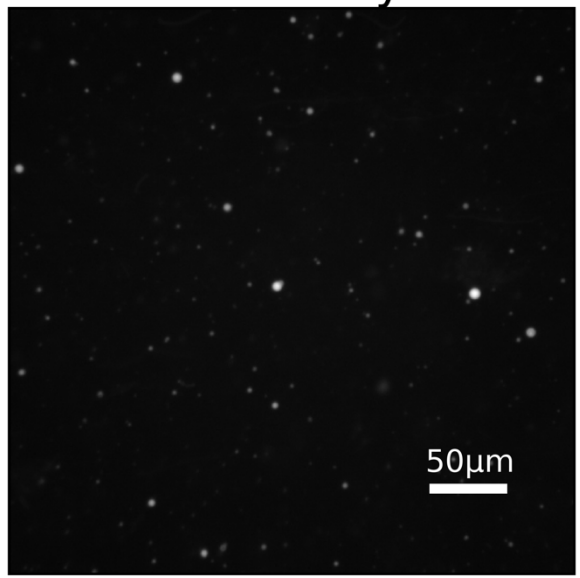


Figure S8: Additional images from the NaCl flocculation experiments shown in Fig 3 ("Flocculate vesicles"). Upon adding enough solid NaCl to saturate the solution, a thick layer of flocculated vesicles can be seen in both test tubes. With 5 mM calcein, the color of the floc layer appears redder than the surrounding solution, suggesting self-quenching of encapsulated calcein. With 0.5 mM calcein, the color of the floc layer appears more similar to the surrounding solution. In both cases, there is a layer of solution containing unencapsulated calcein below the low-density floc layer. At the very bottom of the tube is a layer of undissolved NaCl. See "Experiments on calcein retention during flocculation by saturated NaCl" in the methods section for full details.



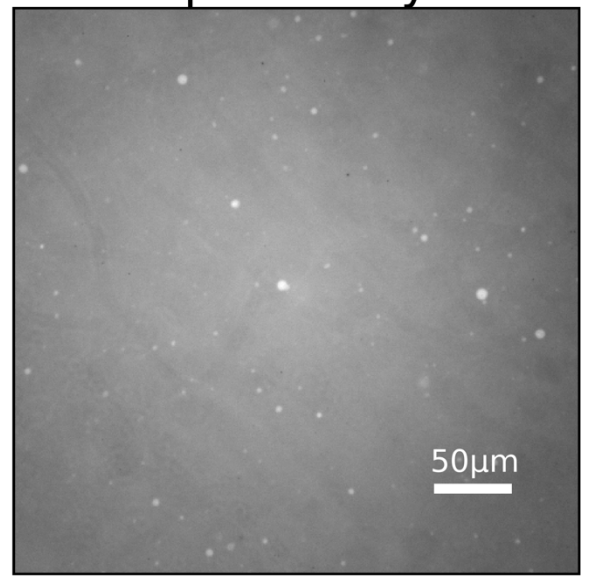


Figure S9: Additional images from the NaCl flocculation experiment shown in Fig 3 ("Disperse vesicles"). See "Experiments on calcein retention during flocculation by saturated NaCl" in the methods section for full details. Scale bars are 50  $\mu$ m.

# Section 3: Additional data from carboxyfluorescein leakage experiments.

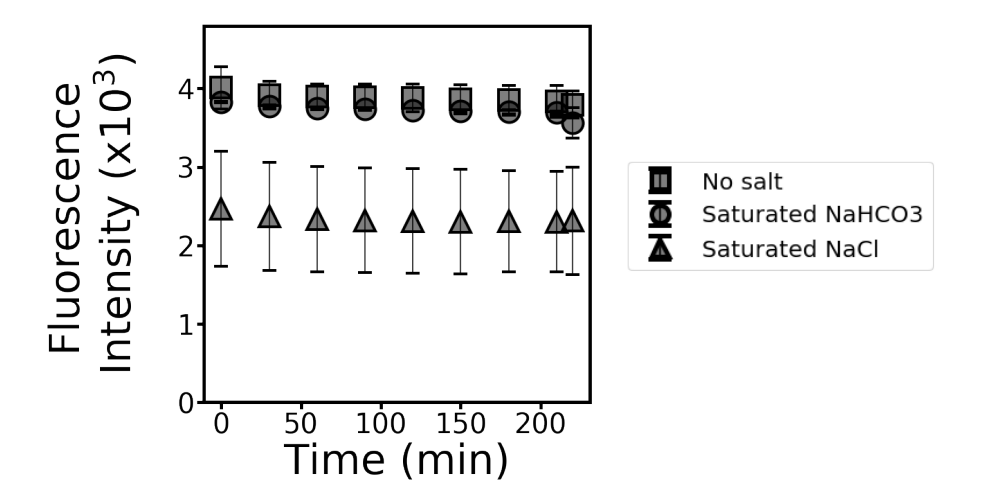


Figure S10: In the absence of vesicles, the fluorescence intensity from 1 mM carboxyfluorescein slightly decreases with time due to photobleaching. Saturated NaCl seems to quench carboxyfluorescein fluorescence. Triton-X-100 is added before the final timepoint, and the result demonstrates that the fluorescence intensity does not change upon addition of Triton-X-100. Error bars represent the standard deviation from two independent experiments.

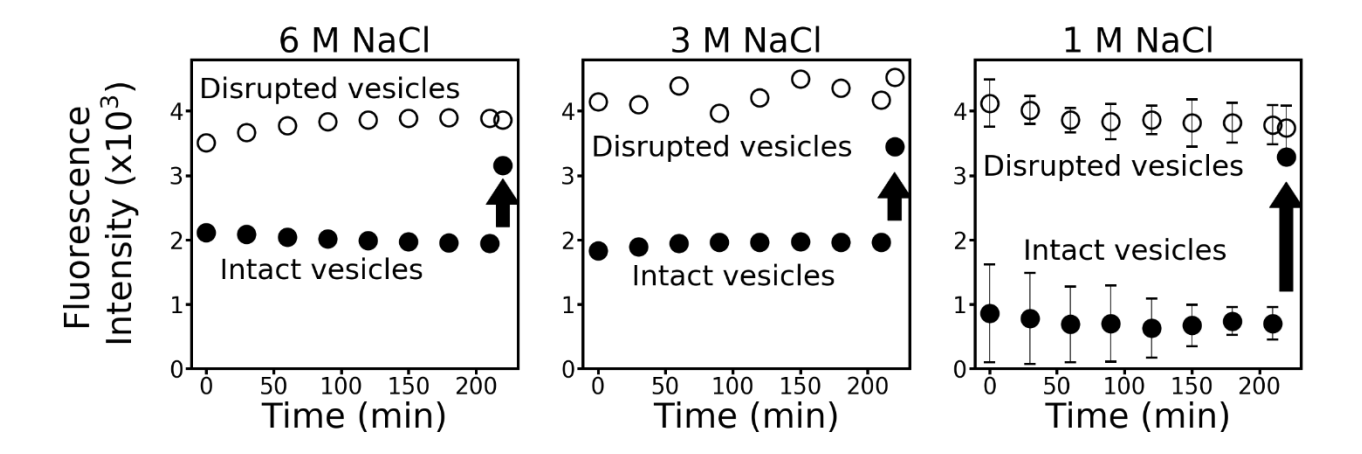


Figure S11: As the concentration of NaCl decreases, the ratio of fluorescence intensities in the disrupted vesicles to the intact vesicles increases. Leakage was monitored through time for flocculated vesicles (filled symbols), and total dye release was induced by Triton-X-100 at the final timepoint (upward arrow). For comparison, total dye release was induced by Triton-X-100 in parallel samples (open symbols). Flocculated vesicles were composed of 2:1 DA: DOH. For the 6 M and 3 M NaCl experiments, the results are for only one experiment each. For the 1 M NaCl experiment, error bars represent the standard deviation from two independent experiments.

# Saturated NaHCO<sub>3</sub>

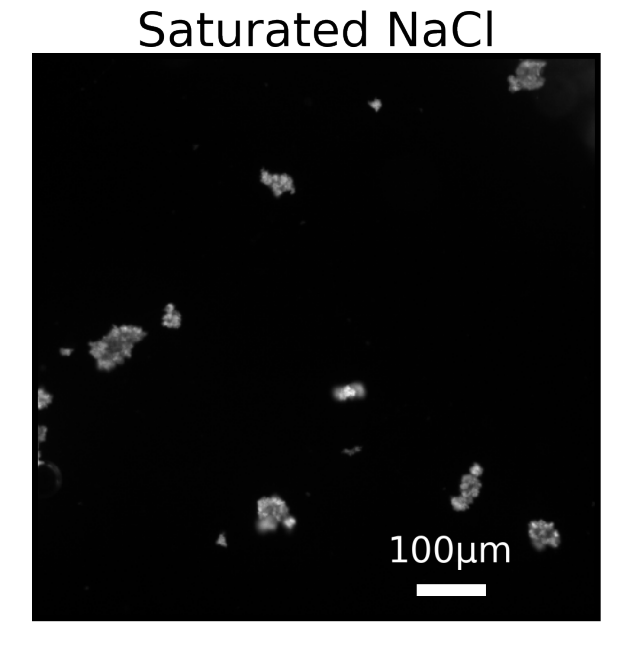
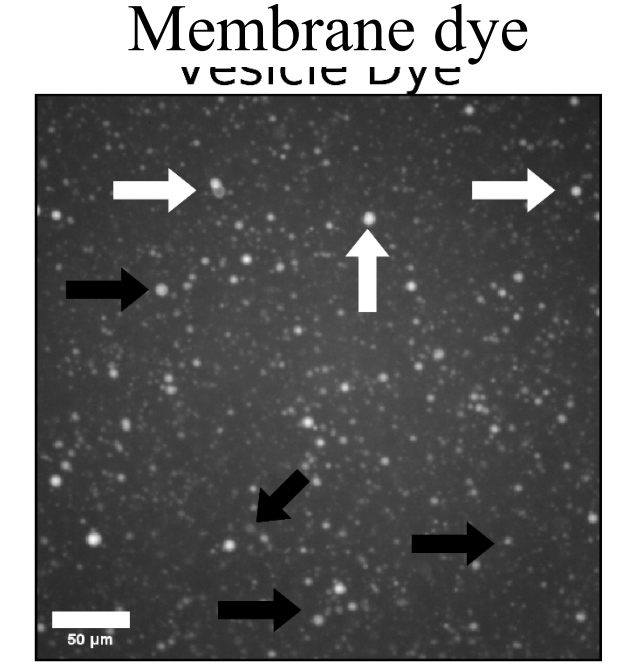


Figure S12: Microscopy confirms that vesicles in saturated salt solution flocculate under the conditions used during Figure 4 experiments. Flocculated vesicles were prepared in the same way as the Figure 4 experiments (see "Experiments on carboxyfluorescein leakage" in the methods section for more details), except that a larger volume of saturated solution was prepared in a test tube, rather than within a 96 well plate. Scale bars are 100  $\mu$ m.

# Section 4: Additional images from dehydration experiments.



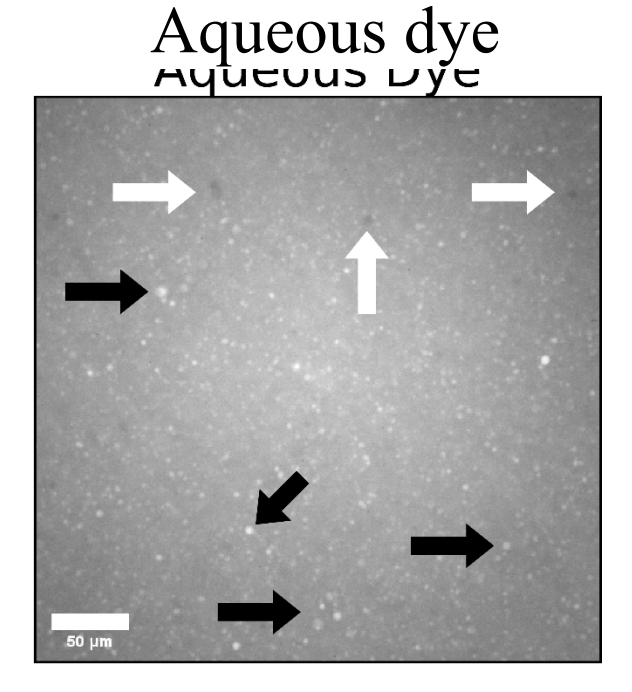


Figure S13: Additional images from the dehydration experiment with fatty acid vesicles composed of 4DA: 1DOH: 1GMD shown in Fig 5 ("Before dehydration"). See "Experiments on calcein retention during dehydration" in the methods section for full details. Black arrows indicate vesicles that are labeled by both the vesicle and aqueous dyes. White arrows indicate vesicles whose calcein florescence is quenched by rhodamine 6G. See Figure S15 for a thorough explanation of this topic. Scale bars are 50  $\mu$ m.

# 50 μm

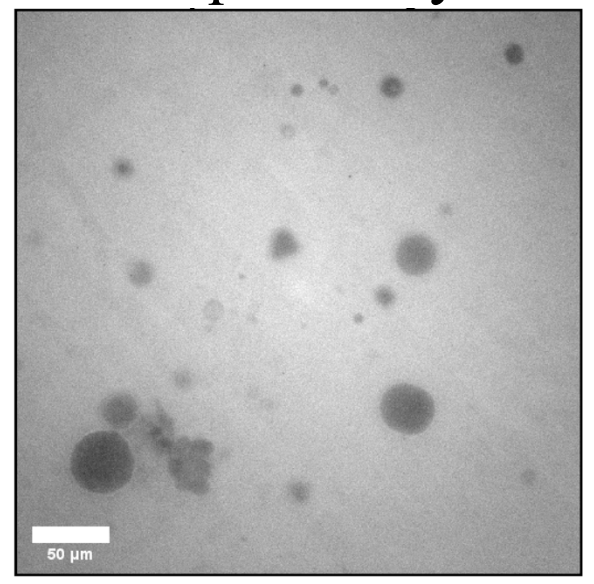
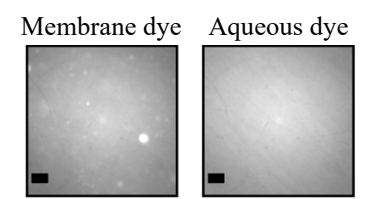
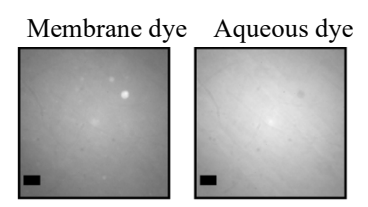


Figure S14: Additional images from the dehydration experiment with fatty acid vesicles composed of 4DA: 1DOH: 1GMD shown in Fig 5 ("After rehydration"). See "Experiments on calcein retention during dehydration" in the methods section for full details. Distinct dark regions in the aqueous dye channel are caused by quenching of calcein fluorescence by rhodamine6G. See Figure S15 for a thorough explanation of this topic. Scale bars are 50  $\mu$ m.

#### 20 µM membrane dye



### 80 μM membrane dye



### 160 μM membrane dye

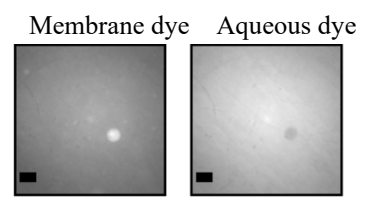


Figure S15: The fluorescence from calcein within vesicles was quenched when the concentration of rhodamine 6G was high. Vesicles were made from 50 mM decanoic acid and 25 mM decanol. The solution inside and outside the vesicles contained 100 mM NaCl, 490  $\mu M$  calcein, and 50 mM bicine. Vesicle aliquots were mixed with different concentrations of rhodamine 6G. At the highest rhodamine 6G concentrations, calcein fluorescence inside the vesicle was quenched. Scale bars are 20  $\mu m$ .

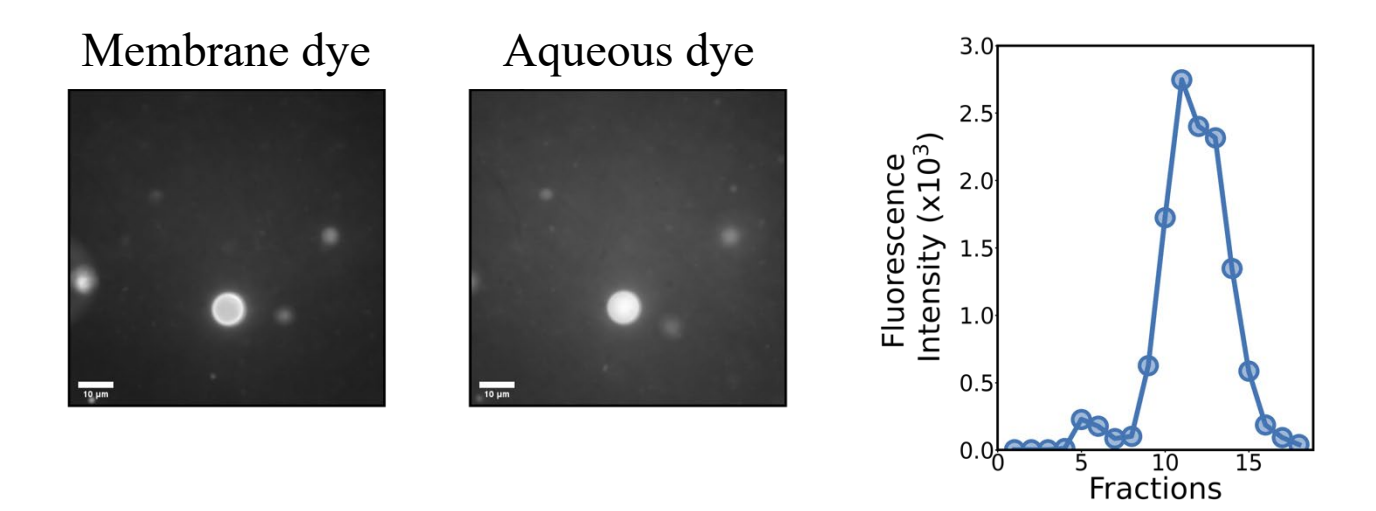


Figure S16: Additional data from the dehydration experiment with fatty acid vesicles composed of 4DA: 1DOH: 1GMD shown in Fig 5. After rehydration, the vesicles were subjected to another round of SEC to confirm that they had indeed re-encapsulated the bulk calcein solution. The SEC chromatogram did show an early-eluting peak corresponding to calcein-containing vesicles, and images of these vesicles confirmed that calcein was encapsulated. See "Experiments on calcein retention during dehydration" in the methods section for full details. Scale bars are 10  $\mu$ m.

# 50 µm

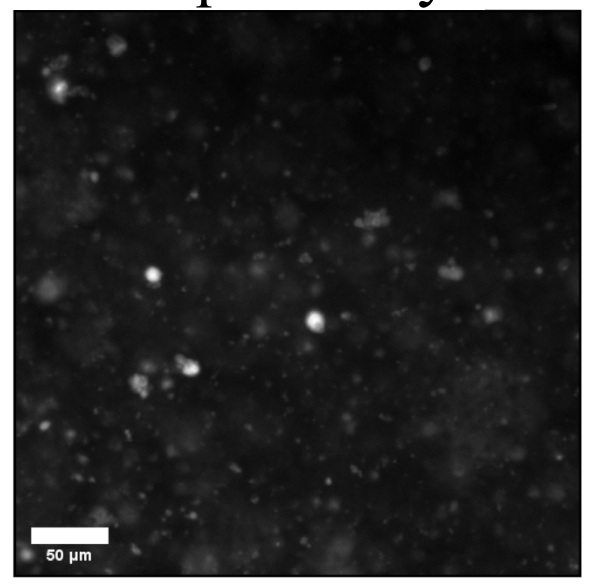
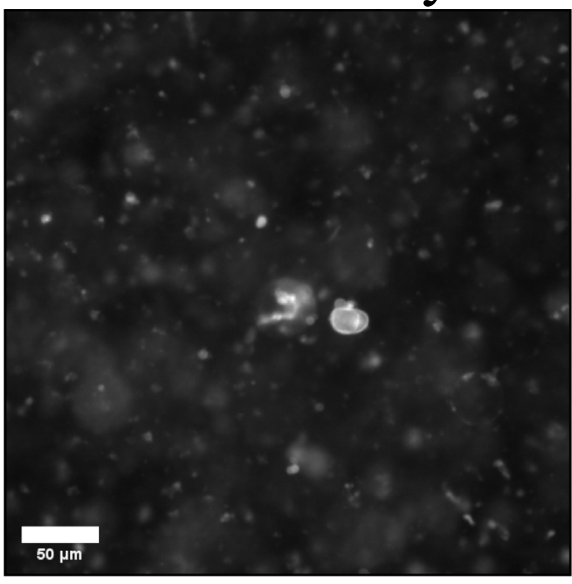


Figure S17: Additional images from the dehydration experiment with phospholipid vesicles composed of 95 mol % DOPC and 5 mol % DOPG shown in Fig 5 ("Before dehydration"). See "Experiments on calcein retention during dehydration" in the methods section for full details. Scale bars are  $50 \, \mu m$ .



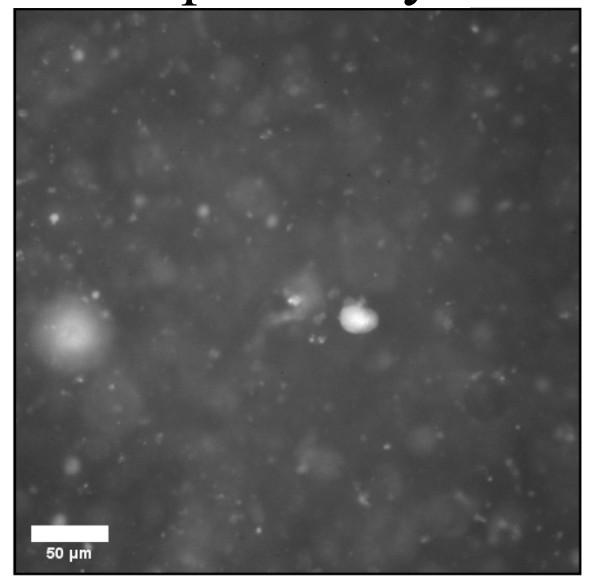


Figure S18: Additional images from the dehydration experiment with phospholipid vesicles composed of 95 mol % DOPC and 5 mol % DOPG shown in Fig 5 ("After rehydration"). See "Experiments on calcein retention during dehydration" in the methods section for full details. Scale bars are  $50 \, \mu m$ .

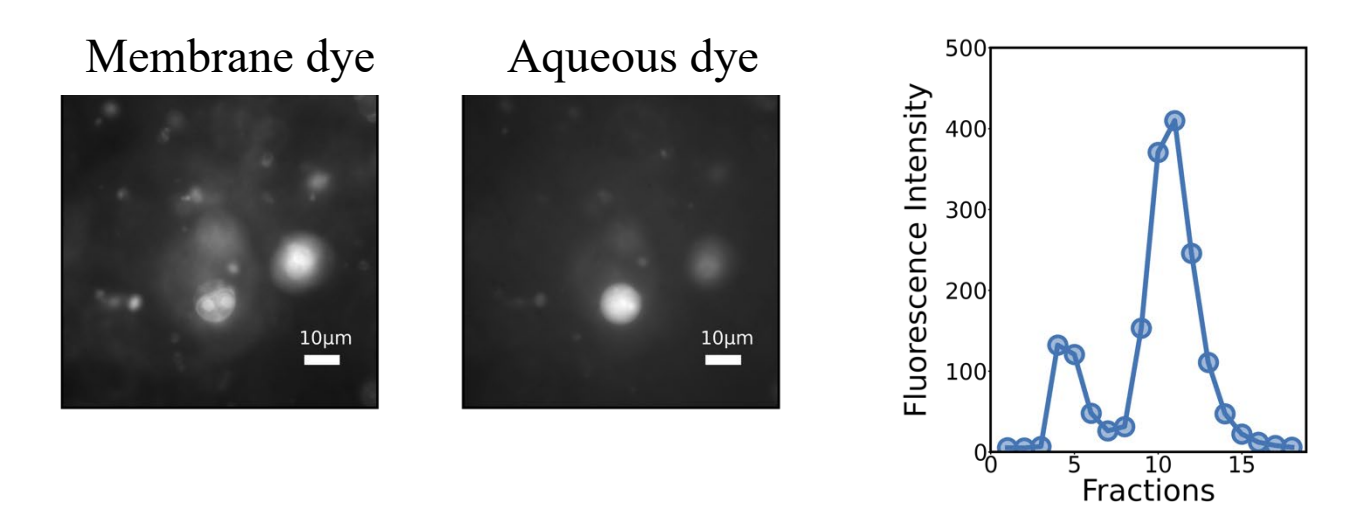


Figure S19: Additional data from the dehydration experiment with phospholipid vesicles composed of 95 mol % DOPC and 5 mol % DOPG shown in Fig 5. After rehydration, the vesicles were subjected to another round of SEC. The SEC chromatogram did show an early-eluting peak corresponding to calcein-containing vesicles, and images of these vesicles confirmed that calcein was encapsulated. See "Experiments on calcein retention during dehydration" in the methods section for full details. Scale bars are 10  $\mu$ m.